Magnetic-field distributions at interstitial sites in nondilute alloys

D. R. Noakes
Physics and Astronomy Department, Brandon University, Brandon, Manitoba, Canada R7A 6A9
(Received 13 May 1991)

Monte Carlo simulations are presented of the instantaneous, dipole magnetic-field probability distribution at an interstitial site in the paramagnetic state of a polycrystalline material involving random alloying of magnetic and nonmagnetic ions on a site, for magnetic concentrations from 1.0 down to 0.03, with particular reference to zero-field (ZF) muon spin relaxation (μSR) in such alloys. In the polycrystalline case, the distribution of local-field magnitudes is more directly related to the ZF μSR than the distribution of field-component values usually discussed. For magnetic-ion concentrations less than about 0.3, the field-magnitude distribution develops a two-site form, and the two types of site are shown to be those with at least one magnetic ion in the nearest-neighbor shell ("high field"), and those with zero magnetic ions in the nearest-neighbor shell ("low field"). Correspondingly, directly simulated static ZF μSR asymmetry spectra develop a two-minimum (two-site) form for the same concentrations. While an approximately Lorentzian component distribution is known to occur in the extreme dilute limit, the approach to that limit from finite concentrations will not be in a simple manner. The high-field distribution must approach that due to a single isolated magnetic moment as concentration decreases, and the low-field distribution evolves from a Gaussian (Maxwellian) shape at its high-concentration (near 0.3) limit toward a more Lorentzian shape. Probability distributions part way between Gaussian and Lorentzian limits are discussed in terms of the Pearson type-VII line shape.

I. INTRODUCTION

Spin-glass behavior has been observed in a wide variety of crystalline alloys in which magnetic ions are randomly distributed on some of the lattice sites (while the rest of the lattice sites are occupied by nonmagnetic ions).[1,2] Positive muon spin relaxation has made notable contributions to the understanding of dilute-alloy spin glasses, using extreme-dilute-limit approximations, such as the assumption that the local-field distribution at the muon position is Lorentzian, when averaged over all sites in the sample.[3–6] Spin-glass behavior is not restricted to dilute alloys, however, and recently data have been collected of muon spin relaxation (μSR) in "diluted magnetic semiconductors" (DMS's), in which the alloyed magnetic ions cannot be considered to be in the dilute limit.[7–10] Analysis of these data has been hampered by the lack of knowledge of what the field distributions at the muons should be, even in principle, even above the freezing temperature T_c, when the magnetic-ion concentration is neither very dilute nor nearly stoichiometric.

Muon spins interacting magnetically with localized moments in a solid material are usually treated in an effective-local-field approximation, in which the moments in the material are considered to cause a magnetic field at the muon site, about which the muon spin Larmor precesses (for a review of the elementary concepts of zero-field (ZF) μSR, see Ref. 11). When the local moments are not in a long-range magnetically ordered state, the local fields at all the muon sites in the sample can be represented by a random local-field probability distribution $P(\mathbf{H})$. Clearly this can be thought of as a joint probability of field magnitude and direction, or as a joint probability of three field components with respect to coordinate axes. In a single crystal, this distribution is likely to be anisotropic with respect to the crystal symmetry axes. but the vast majority of μSR experiments are performed on polycrystalline samples, in which only averages over anisotropies in properties can be measured. The work presented in this article concerns only this polycrystalline case. In such a sample, the single-crystal-field distribution for the material becomes "polycrystal averaged," becoming a field-magnitude distribution $P(|\mathbf{H}|)$ (multiplied by a constant orientation probability distribution), or the joint probability of field components in three equivalent orthogonal directions. It is often assumed that this joint component probability factors into the product of three identical component distributions $P(H_i)$, but this is not always the case.

From the probability distribution, the (ZF) muon spin relaxation function, usually labeled $G_{zz}(t)$, which is proportional to the muon ensemble polarization as a function of time (measured from the moment each muon stops at its site), can in principle be calculated. In the case of a stationary muon and static moments, the calculation is the averaging of the Larmor precession at every possible field over the probability distribution. When the muon moves from site to site, or when the moments themselves are fluctuating, the relaxation function also depends on the details of the fluctuation process(es), which this article is not concerned with. Since there is a one to one correspondence between field distribution and static relaxation function, it is instructive to see the effect of a change in the former on the latter. Unfortunately, there are only two accepted "realistic" random-local-field distributions and associated static relaxation functions that are analytically specified: the Gaussian distribution expected to occur when there is a dense array of essen-

tially equivalent moments, and the Lorentzian mentioned above in the extreme dilute moment limit.[11,12] Both of these are idealizations in that they take no account of the lattice periodicity of crystalline solids, representing moment distances from the muon site by a continuum instead. The associated "Kubo-Toyabe" relaxation functions,[13,3,14] with elaborations representing the effects of fluctuations, have been remarkably versatile in their ability to reproduce observed ZF μSR data in magnetically disordered states, but there is a question of when deviations from the idealizations might be detectable.[15] In the case of alloying magnetic ions with nonmagnetic ones in a material, if the complete concentration range is allowed, the local-field distribution can at best take on the two limit cases at the two limits of concentration, and must evolve from one to the other as a function of magnetic concentration between the two limits. This evolution has not previously been studied.

To properly include effects of lattice periodicity, it is usually necessary to consider particular crystal structures individually, although results may then become material specific. When looking for corrections to the effective-field approach by a completely quantum calculation, fcc copper metal was the experimentally motivated choice, but only a small number of copper ions nearest the muon site could be handled.[16,17] Since in that case the effective-local-field concept was explicitly abandoned, the ZF relaxation function was calculated directly from the microscopic interaction of muon spin with a small cluster of ion spins. Meanwhile, if the local-field approximation is retained, it has been shown that, given any particular random-field distribution, the associated relaxation function can be well simulated by a Monte Carlo procedure.[18] In the same spirit, given a crystal structure [with identified muon site(s)] and a particular effective-field mechanism (an expression for calculating the field at the muon site due to a lattice moment), the random-field distribution for the magnetically disordered state can also be simulated by Monte Carlo.[19]

This paper presents results of Monte Carlo modeling of polycrystal-averaged dipole-field distributions, averaged over all sites in a sample, for the octahedral interstitial site in the fcc (e.g., copper) lattice, as a function of the concentration of randomly alloyed magnetic ions (e.g., manganese), treated as classical dipole moments, from 3% to 100%, with no orientational correlation between moments. This distribution should apply to the paramagnetic state (where there will be rapid fluctuations), and also to the low-temperature frozen spin-glass state, should it occur with no moment-moment correlations. The fcc lattice, with consideration of only one crystallographic muon site, and the restriction to dipole coupling of the moments to the muon, provide relative computational simplicity and some contact with experiment at low concentration. In the true Cu(Mn) system, band magnetism effects [such as the Ruderman-Kittel-Kasya-Yosida (RKKY) interaction] clearly act between manganese moments, and at high concentrations cause long-range magnetic order, but it is believed that muon spin relaxation is dominated by dipole coupling at low concentrations.[20] In the DMS that originally motivated this work, the crystal structure requires that there be at least two distinct muon sites,[10] and there may be superexchange bond polarization effects at the muon site. Pure dipole coupling may apply to insulator spin glasses, but again these have more complicated crystal structures.

In Sec. II, ways of parametrizing random-field distributions relative to the two idealizations are discussed. In Sec. III, the computational method is described and the calculated field distributions are presented. In Sec. IV, possible physical interpretation of the Monte Carlo results will be developed. Section V presents conclusions.

II. CHARACTERIZATION OF FIELD DISTRIBUTIONS

It has been found that in almost all cases where the ZF bare muon (not muonium) spin-relaxation signal has been resolved in a static system of concentrated, but not magnetically ordered, moments (typically polycrystalline metallic samples containing only nuclear moments), it has conformed closely to the "static Gaussian Kubo-Toyabe" relaxation function[21,22] (the notable exception occurs in coupling to fluorine moments[23,24]). The interpretation of this is that the moments generate an effective classical magnetic field at each muon site, where each of the three field components is randomly (and independently) chosen from a Gaussian probability distribution. For a polycrystalline solid, with Cartesian axes defined with respect to the muon beam polarization direction (not the local crystallite axes), or in a single crystal if there happens to be no anisotropy,

$$P^G(H_i)=\frac{1}{\sqrt{2\pi}\sigma}\exp\left[-\frac{H_i^2}{2\sigma^2}\right], \quad i=x,y,z , \tag{1}$$

where σ is the root-mean-square (rms) field component. This corresponds to a Maxwellian distribution of field magnitudes:

$$P^G(|\mathbf{H}|)=\left[\frac{2}{\pi}\right]^{1/2}\frac{|\mathbf{H}|^2}{\sigma^3}\exp\left[-\frac{|\mathbf{H}|^2}{2\sigma^2}\right] . \tag{2}$$

The Larmor precession of each muon spin around its local field then generates the static zero-applied-field Gaussian Kubo-Toyabe "relaxation" of the muon ensemble polarization (by dephasing, also called inhomogeneous broadening):

$$G_{zz}(t)=\tfrac{1}{3}+\tfrac{2}{3}\int P(|\mathbf{H}|)\cos(\gamma_\mu|\mathbf{H}|t)d|\mathbf{H}| , \tag{3}$$

where $\gamma_\mu=2\pi(1.355\times10^4\ \mathrm{s}^{-1}\,\mathrm{Oe}^{-1})$ is the magnetogyric ratio of the muon. For the Gaussian case

$$G_{zz}^G(t)=\tfrac{1}{3}+\tfrac{2}{3}(1-\Delta^2t^2)\exp\left[-\frac{\Delta^2t^2}{2}\right] , \tag{4}$$

where $\Delta=\gamma_\mu\sigma$.

For infinitely dilute local moment impurities in a host, on the other hand, it has been shown[12] that the local-field distribution at a site should be Lorentzian:[3-6]

$$P^L(H_i)=\frac{1}{\pi W}\frac{1}{(1+H_i^2/W^2)} , \quad i=x,y,z \tag{5}$$

$$P^L(|\mathbf{H}|)=\frac{4}{\pi W}\left[\frac{|\mathbf{H}|^2}{W^2}\right]\frac{1}{(1+|\mathbf{H}|^2/W^2)^2}\ , \tag{6}$$

where W is the component distribution half width at half maximum (HWHM). To distinguish between $P^L(H_i)$ and $P^L(|\mathbf{H}|)$ in words, the latter may be called "the magnitude Lorentzian." In the same manner as Eq. (4), this distribution generates the static "Lorentzian Kubo-Toyabe" ZF relaxation function:

$$G_{zz}^L(t)=\tfrac{1}{3}+\tfrac{2}{3}(1-at)\exp(-at)\ , \tag{7}$$

where $a=\gamma_\mu W$. The Gaussian and Lorentzian cases are compared in Fig. 1. Whereas the primary characterization of component distributions is in terms of widths, vector-magnitude distributions have variable most probable fields, H^*, as their foremost feature. Therefore, the component distributions [Fig. 1(a)] have been drawn with equal widths at half maximum ($W=\sqrt{2\ln 2}\sigma=1$), but the magnitude distributions [Fig. 1(b)] with equal peak positions ($W=\sqrt{2}\sigma=1$), and the static ZF relaxation functions [Fig. 1(c)] with the same parameters as the magnitude distributions.

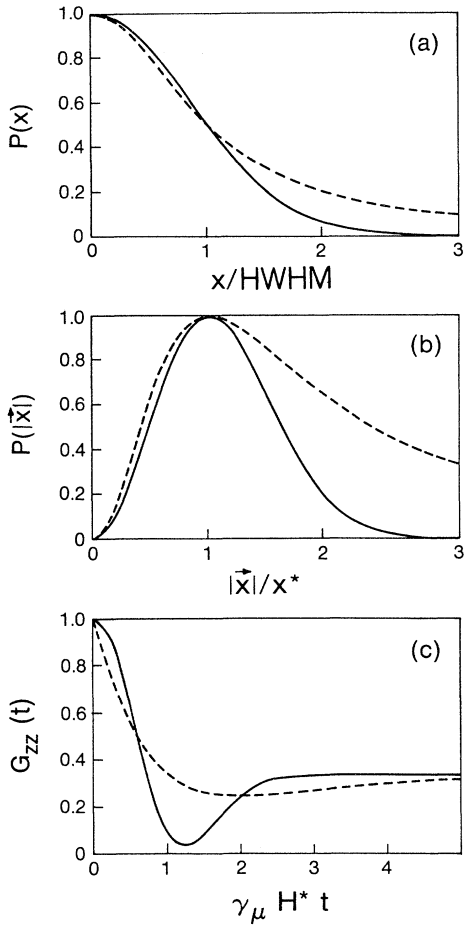

FIG. 1. Comparison of Gaussian (solid lines) and Lorentzian (dashed lines) (a) component probability distributions, (b) vector-magnitude probability distribution, and (c) static zero-field Kubo-Toyabe spin relaxation functions.

The pure Lorentzian distribution is known to be somewhat pathological, in that the nontrivial moments of the distribution

$$\langle (H_i)^{2m}\rangle=\int_{-\infty}^{\infty}(H_i)^{2m}P(H_i)dH_i\ ,\quad n=2m\ \text{(even)} \tag{8}$$

$$\langle |\mathbf{H}|^n\rangle=\int_0^\infty |\mathbf{H}|^n P(|\mathbf{H}|)d|\mathbf{H}| \tag{9}$$

diverge for all $n>0$ (Ref. 25) [hence there is no rms field to use in the definition, Eqs. (5) and (6)], while all the moments of the Gaussian distribution are finite. This is in fact due to the continuum approximation: there is no upper bound on the field at the site, which in terms of the physical model of fixed-magnitude moments means that there is no lower bound on the distance between the muon and a moment. In reality, the positive muon will not get closer to an ion than the chemical ionic radius (or sometimes a bond radius, depending on the chemical interactions). For each particular muon site in a crystalline lattice, this distance can be called the nearest-neighbor (NN) distance. Both the Gaussian and the Lorentzian distributions allow arbitrarily large local fields to occur. But the exponential high-field decay of the Gaussian probability keeps the moments of the distribution finite and reasonable. It is possible to modify the Lorentzian to induce it to have finite moments, by cutting off the probability at some field value H_c corresponding to the effect of moments in the NN shell (and setting the probability to zero for all larger fields), for example, but then the finite moments that result are all explicitly dependent on the value of the cutoff field, which becomes a new parameter of the theory. Other methods of modifying the Lorentzian to make it more physically reasonable are also possible.[25] The difference in predicted relaxation function caused by somehow reducing the high-field probability to get finite moments is known to be primarily in the very early part of the relaxation [times of order $1/(\gamma_\mu H_c)$]. In particular, the static Lorentzian Kubo-Toyabe function has negative slope at $t=0$, whereas a realistic field distribution should cause a static relaxation function with zero slope at $t=0$.[18] If data are taken at time resolution much more coarse than $1/(\gamma_\mu H_c)$, however, the only clearly established problem caused by fitting the pure Lorentzian Kubo-Toyabe to real data is a systematic overestimate of the initial asymmetry (of the polarized muon decay positron (parity-violating) direction).

The evaluation of moments of a numerically generated probability distribution is straightforward, and involves no modeling beyond that which generated the distribution. When the calculation uses a finite cluster of magnetic moments, however, the distribution moments deduced will be consistently less than the true values for the material, and some estimate of the size of the systematic error should be made, usually by noting the effect of changing cluster size. For comparison to the numerical simulation moments, the Gaussian distribution's (well-known) moments are

$$\langle (H_i)^{2m}\rangle_G=(2m-1)!!\sigma^{2m}\ , \tag{10}$$

$$\langle |\mathbf{H}|^{2j}\rangle_G=(2j+1)!!\sigma^{2j}\ ,\quad n=2j\ \text{(even)} \tag{11}$$

$$\langle |\mathbf{H}|^{2j+1} \rangle_G = \left[\frac{2}{\pi} \right]^{1/2} 2^{(j+1)}(j+1)!\sigma^{(2j+1)} ,$$

$$n = 2j+1 \text{ (odd)} . \quad (12)$$

Note that if the three selections of component field value (to make a complete specification of $\mathbf{H}$) from the component distributions are statistically independent, then $\langle |\mathbf{H}|^2 \rangle$ will equal $3\langle (H_i)^2 \rangle$. If the three selections are not independent, those two values need not even approximate each other. As an extreme example of this, consider the field distribution in which the magnitude of the local field is constant at value H_0, but its orientation is isotropically random (this is the simplest possible case of ZF μSR in a polycrystal ferromagnet when the sample has no net magnetization). It is easy to see that the component field distribution is ellipsoidal,

$$P^F(H_i) = \frac{2}{\pi H_0} \left[1 - \frac{H_i^2}{H_0^2} \right]^{1/2} , \quad -H_0 \le H_i \le H_0 \quad (13)$$

while the magnitude distribution, $P^F(|\mathbf{H}|)$, is a δ function. Then $3\langle (H_i)^2 \rangle = 3H_0^2/8$ while $\langle |\mathbf{H}|^2 \rangle = H_0^2$. The corresponding muon polarization function does not relax at all, it is a cosine in time with frequency $\gamma_\mu H_0$, which is clearly derivable from $P^F(|\mathbf{H}|)$, but not so directly from $P^F(H_i)$.

III. THE MONTE CARLO CALCULATION

Calculations were performed on a cluster of 490 ions in the fcc structure, centered on the octahedral interstitial site (the most likely muon site in copper). The cluster is spherical in the sense that it includes all ions inside a radius slightly more than three cubic unit-cell axis lengths, corresponding to about 11 Å in pure copper at room temperature (and no ions outside that). For each magnetic ion concentration chosen from the range $0.03 < x \le 1$, for each iteration (evaluation of the total field at the center), that proportion of fixed-magnitude (Mn^{3+}, $5.0\mu_B$) magnetic moments was distributed by a pseudorandom number routine over the ion positions of the cluster, and the orientation of each moment was chosen pseudorandomly. Additionally, the orientation of the crystal axes of the cluster with respect to the external laboratory coordinates was chosen pseudorandomly (this is the polycrystal averaging), in each iteration. The sum over the cluster of the dipole field at the center was evaluated, and its three components with respect to laboratory Cartesian coordinates and its magnitude were stored in histograms with up to 200 bins across the range of field value encountered (an early version of this program was described in Ref. 15). Typically several tens of thousands of iterations were performed for each value of x. The lowest nontrivial moments of the field distributions were evaluated by summing over the histograms.

For a selection of concentrations, the summed magnetic field at the site was used to explicitly precess a classical dipole muon spin from $t = 0$ (pointing along the laboratory z axis) until decay, and the spin component along the z axis at decay was recorded in a time histogram, to build up a direct numerical simulation of the static zero-field muon spin relaxation function that would be observed in experiment (the basic numerical μSR relaxation function Monte Carlo program used was originally written by Brewer[18]). This direct simulation is computationally very slow, and so was only done in a couple of test cases, at lower statistics than the field distribution simulations. Thus claims made about relaxation functions based on analysis of the field distributions calculated were testable by comparison to a small number of complete simulations of the relaxation that did not interrupt the microscopic process in its middle to deduce the field distributions.

Note that, with a cluster of this size, concentrations below a value between $x = 0.02$ and 0.03 cannot be handled because the moment assignment procedure then begins to assign zero magnetic moments to the cluster in a significant fraction of the iterations. No attempt was made to directly include the effect of ions outside the cluster. These may well affect the overall scale of the distributions, and may have increasing proportional effect as x decreases, but they are unlikely to affect the qualitative phenomenology presented below, which was found to depend primarily on the detailed magnetic occupancy of the nearest-neighbor shell.

The calculated field-magnitude distributions for a selection of concentrations are shown in Fig. 2 and the corresponding directly simulated static muon polarization relaxation functions are shown in Fig. 3. The corresponding component distribution at each x from 1.0 down to near 0.5 was well fit by a single Gaussian with rms field component decreasing as concentration decreases. Below $x = 0.5$ the field-component distribution developed wings that could only be fit by a more complicated function, such as the sum of two Gaussians (both centered on field-component value zero) with different widths. When the total field distribution is the sum of two distinct terms, the relaxation function should be the sum of the relaxation functions due to the two terms separately. Prediction from such fits then that the relaxation function would develop a two-minimum form at concentrations up to nearly 0.5 were not confirmed by the direct simulations, so it appears difficult to relate the component distribution to the true relaxation function. The magnitude distribution had form fairly well fit by a single Maxwellian down to at least $x = 0.4$, but at $x = 0.3$ had developed a shoulder on the low-field side of the main peak, and clearly became a two-peak distribution by $x = 0.25$ (see Fig. 2). The directly simulated relaxation functions correspondingly did develop a two-minimum form between $x = 0.3$ and $x = 0.2$. Thus the deduced field-magnitude distribution is at least qualitatively correlated with the relaxation function, but the component distribution is not (and this is why the component distributions have not been presented in figures). This discrepancy may be due to lack of statistical independence in the random selection of the three component values, but since the value of $3\langle (H_i)^2 \rangle$ as a function of x only deviated from $\langle |\mathbf{H}|^2 \rangle$ by a maximum of 5% (and the numerical uncertainty in the values is of order 2%), it is not completely clear that this is the problem. Note that in Fig. 3, the solid lines were generated at late times by smoothing over statistical jitter, using the knowledge that G_{zz} must settle down to the value $\frac{1}{3}$ at late times.

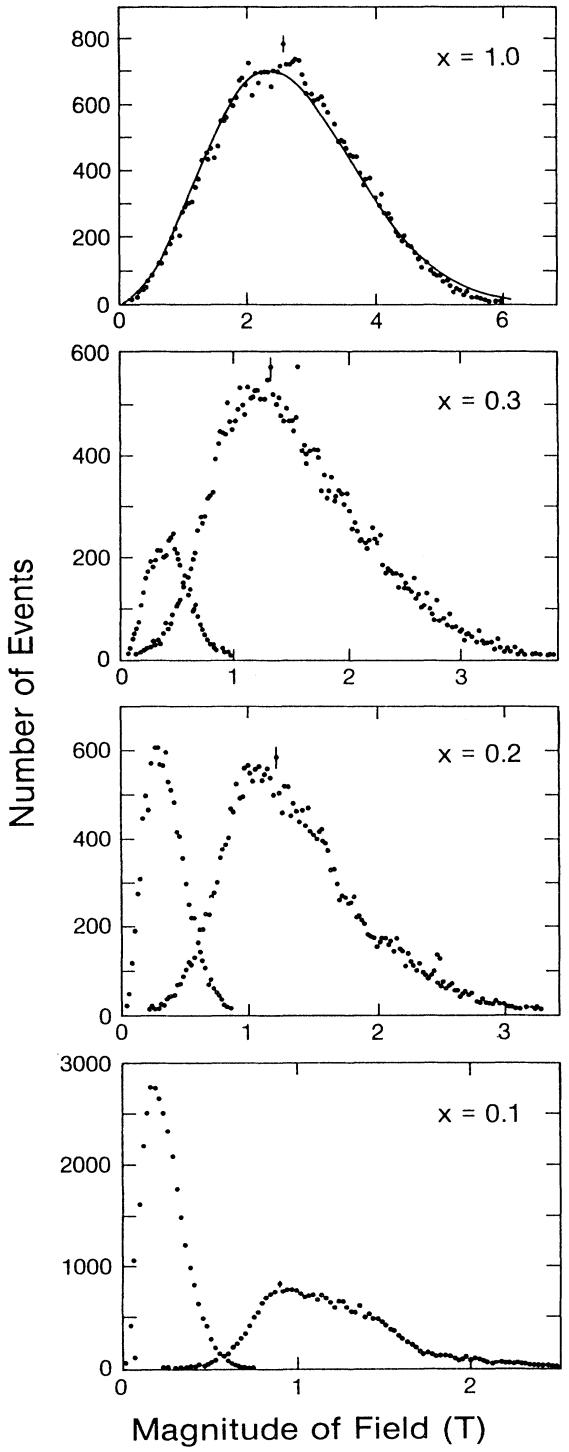

FIG. 2. Monte Carlo dipole field-magnitude distributions at the octahedral interstitial in fcc $Cu_{1-x}Mn_x$, for concentrations x as indicated. In the lower three frames, the distribution which peaks at a higher field is that for sites around which the nearest-neighbor shell contains at least one magnetic ion, while the lower-field distribution is for sites around which the NN shell is empty of dipoles. The total distribution is the sum of the two. The solid line in the $x = 1.0$ frame is the least-squares-fit Maxwellian. Representative $\sqrt{n}$ error bars are shown in each frame.

The most common cause of a sum of two-term field distribution is the existence of two distinct occupied muon sites in the sample, and while the muon site in the cluster was chosen to be crystallographically unique, it need not then be magnetically unique. After the observation of the two-peak form of the magnitude distributions for $x \leq 0.25$ the Monte Carlo program was modified to store the field for iterations in which the NN shell around the site (six ions) happens to be assigned at least one magnetic moment in a separate histogram from those iterations

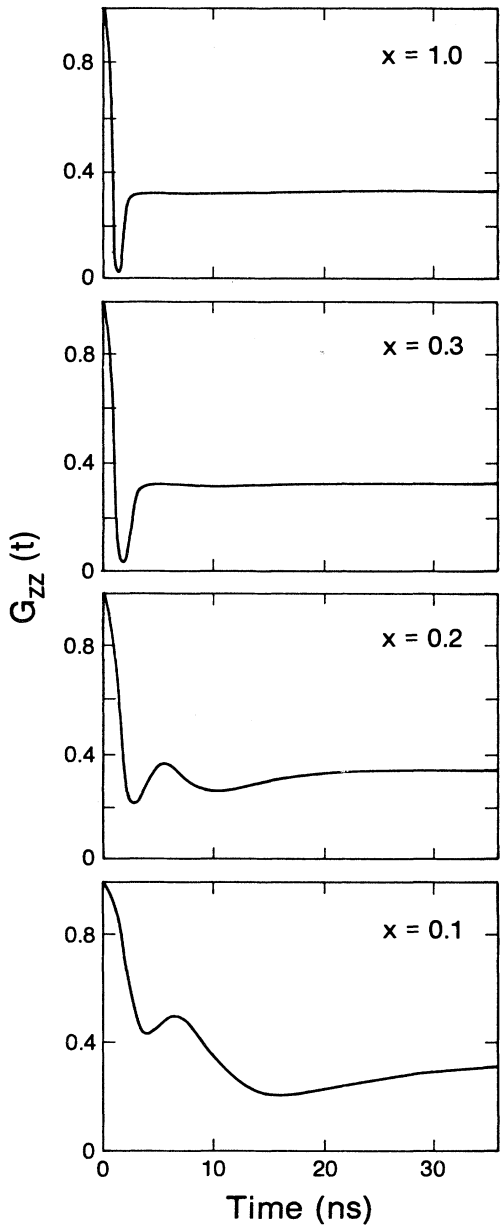

FIG. 3. Monte Carlo static ZF muon spin (polarization) relaxation functions generated by the random dipole field distributions at the octahedral interstitial in fcc $Cu_{1-x}Mn_x$, for concentrations x as indicated. The solid lines were generated by drawing a smooth line through the statistical jitter of the simulation.

in which the NN shell happens to be assigned zero magnetic ions. This "NN-shell separated" field-magnitude distribution, for particular values of x, is what is shown in Fig. 2. The total distribution is the sum of the two parts in each frame of Fig. 2, and the interpretation is now clear.

Below concentration about 0.3, there are two magnetically distinct muon sites in the sample. The "high-field site" is the one for which there is at least one magnetic nearest neighbor. The "low-field site" is the one for which the NN shell is completely nonmagnetic. The latter is not seen at higher concentration because it simply has too small probability of occurrence: $(1-x)$ to the power of the number of ions in the shell (6, in this case). The nearest magnetic ion is then at least the next-nearest-neighbor (NNN) distance away, and its field at the site relative to the effect of the NN magnetic ion on the high-field site is in the ratio of the distances ($\sqrt{3}$ in fcc) to the power 3.

As concentration decreases further below 0.3, the percentage of high-field sites in the sample decreases in favor of the low-field site. While this is happening, the peak of the high-field distribution (its most probable field magnitude, H^*) decreases only slightly. Additionally, the high-field distribution develops a nonzero minimum field magnitude, which increases as x decreases. The field-magnitude distribution for $x=0.05$ is shown in Fig. 4. In the extreme low-concentration limit, the shape of the high-field distribution (separate from its amplitude relative to the low field, which goes to zero in this limit) should approach that for a single classical magnetic dipole one NN distance away from the interstitial site, with random orientation with respect to the separation vector. The form of this is mathematically related to that of Eq. (13), in that the ellipse of Eq. (13) is now cut off at a minimum field magnitude of $H_0/2$ (which is then H^*):

$$P^D(|\mathbf{H}|)=\frac{4}{(2\pi/3-\sqrt{3}/2)H_0}\left[1-\frac{|\mathbf{H}|^2}{H_0^2}\right]^{1/2},$$
$$\frac{H_0}{2}\le|\mathbf{H}|\le H_0\ . \quad (14)$$

For the cluster and moments used in this study, H_0 should be near 1.6 T, with which Fig. 4(b) is consistent. The equation is the $x\to 0$ limit form of the high-field part of the distribution in the (semiclassical) effective-field approximation. If the interaction of a muon with a single other moment is thought to be detectable, however, it should probably be dealt with in a more exact quantum treatment. Meanwhile, down to the lower limit of concentration due to the finite cluster size (about 0.03) the low-field distribution retains a single-peak form with the peak position decreasing as concentration decreases.

How then might the field distributions of Figs. 2 and 4 approach anything resembling a magnitude Lorentzian [Eq. (6)] as concentration goes to zero? The nth moment of a distribution can be expressed as "the nth-order characteristic field" by taking the nth root: $\langle|\mathbf{H}|^n\rangle^{1/n}$. First order is the average field magnitude and second order is the rms field magnitude, and these lowest two, divided by the rms field magnitude at $x=1.0$ (2.79 T) to make them dimensionless, are shown in Fig. 5. In spite of the complicated phenomenology of Figs. 2 and 4, all

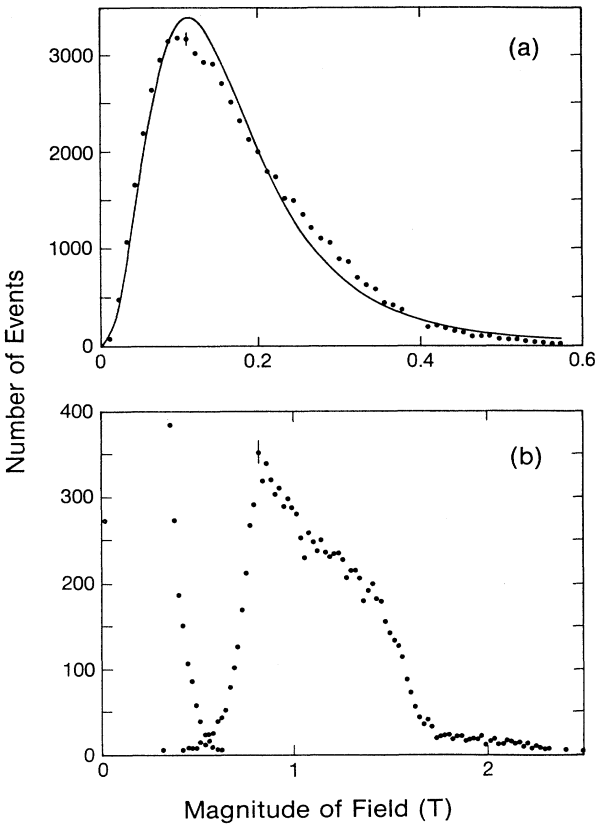

FIG. 4. Monte Carlo dipole field magnitude distribution at the octahedral interstitial in fcc $Cu_{0.95}Mn_{0.05}$: (a) for sites around which the nearest-neighbor shell contains zero magnetic ions, and (b) for sites around which the NN shell contains at least one magnetic ion, superimposed on the tail of (a). The total distribution is the sum of the two. This concentration is near the limit of validity of the calculation, and may be inaccurate near $|\mathbf{H}|=0$. The solid line in (a) is the least-squares fit of the "magnitude-Pearson" function described in the text. Representative $\sqrt{n}$ error bars are shown in each frame.

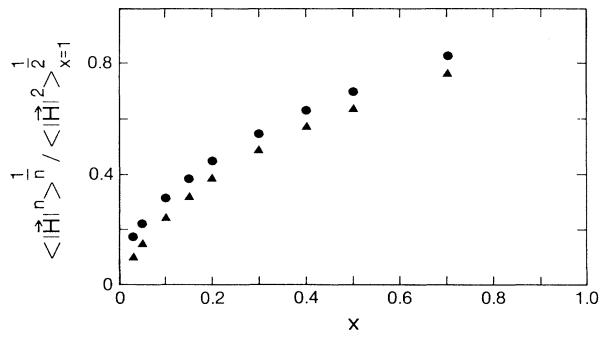

FIG. 5. The average, $\langle|\mathbf{H}|\rangle$ (triangles), and rms, $\sqrt{\langle|\mathbf{H}|^2\rangle}$ (circles), fields of the Monte Carlo field-magnitude distributions in fcc $Cu_{1-x}Mn_x$, divided by the value of the rms magnitude at $x=1$, as a function x.

moments tabulated were found to decrease smoothly as a concentration decreases. They *must* decrease because magnetic moments are being removed from the material, and they must become zero as concentration goes to zero, as long as the muon does not preferentially trap near magnetic ions as it stops in the material. The Monte Carlo distribution moments cannot approach the pure Lorentzian's divergent moments because the latter are artifacts of the continuum approximation as discussed above. The mean-square field magnitude $\langle |\mathbf{H}|^2 \rangle$ is essentially linear in x, which means that it is simply proportional to magnetic moment per unit volume.

It is also possible to compute ratios of different-order characteristic fields for a distribution and compare them to those of other distributions. Figure 6 shows that the ratio of rms to average Monte Carlo alloy field magnitudes is roughly linear in $1/x$, over the range of concentration studied. The value of this ratio for the Maxwellian distribution is $\sqrt{3\pi/8}$, a value which the Monte Carlo distributions remain near for $0.5 \leq x \leq 1$. Meanwhile, since each successive Lorentzian moment diverges more strongly than the one before it, the ratio of any higher-order–to–lower-order characteristic field also diverges for the magnitude-Lorentzian distribution. Since the ratio shown in Fig. 6 increases as x decreases and could conceivably diverge as x tends to zero, the distribution moments may be approaching those of the Lorentzian in this sense.

It is also interesting to consider how the relaxation functions themselves approach the Lorentzian Kubo-Toyabe form as concentration goes to zero. Figure 7 shows the directly simulated zero-field muon relaxation function for $x = 0.05$ (solid line), and the least-squares fit of a Lorentzian Kubo-Toyabe to the simulation for times greater than 7 ns (dotted line), which has been extrapolated back to zero time to show the overestimate of initial asymmetry mentioned above. All time differential μSR data exhibit gaps between the muon stop ($t = 0$ by definition) and the earliest good data bins, for instrumental reasons. A 7-ns "dead time" is near the minimum achieved in typical experiments (see, for example, Ref. 26). With the first minimum of the relaxation function lost in such a dead time, the detectable part is fit reasonably well by the Lorentzian Kubo-Toyabe. Low-amplitude high-frequency oscillations due to the high-field site's narrow field distribution, visible in Fig. 7, may be an artifact of the semiclassical approximation used, as a full quantum treatment is likely to result in more complicated relaxation behavior for the high-field site. To fit the complete relaxation function from $t = 0$, generally the high-field site effect must be represented as a coherent, relaxing, oscillation. A high-field Gaussian Kubo-Toyabe summed with either a low-field Gaussian Kubo-Yoyabe or a low-field Lorentzian Kubo-Toyabe results in a much poorer fit to $x = 0.05$ (the same is true for $x = 0.1$).

As a simple test of the error caused by using a finite cluster, Monte Carlo runs were repeated using only the central core of the cluster, out to a radius of $\frac{1}{2}$ the full cluster radius (thus $\frac{1}{8}$ of the volume, in this case containing 68 ions), for concentrations for which the numerical calculation will not assign zero ions to the cluster a significant number of times (this requires x larger than some number between 0.1 and 0.15). The resulting field distributions were nearly indistinguishable by eye from those shown in Fig. 2, and the low-order distribution moments evaluated by summing were smaller by typically 1% for the same cluster than for the large. Thus the core of half the radius of the full cluster used is essentially responsible for the distributions calculated, and the outer $\frac{7}{8}$ of the cluster causes 1% changes, until the concentration falls too low to be accurately represented by the core alone.

IV. DISCUSSION

The development of two distinct, comparably populated sites for $0.3 \geq x \geq 0.1$ is a feature of the results not predicted beforehand. It indicates that the information

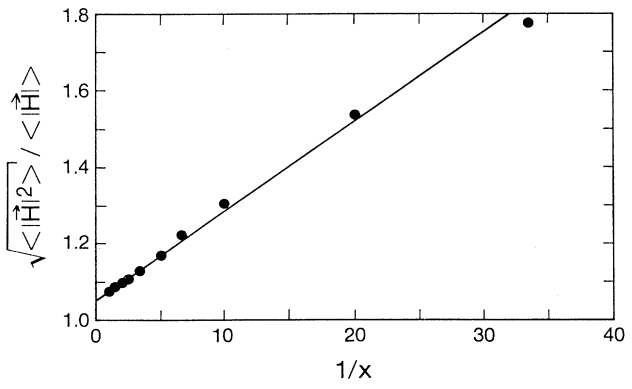

FIG. 6. The ratio of the rms to average Monte Carlo field magnitude in fcc $Cu_{1-x}Mn_x$ vs $1/x$. The straight line is a guide to the eye.

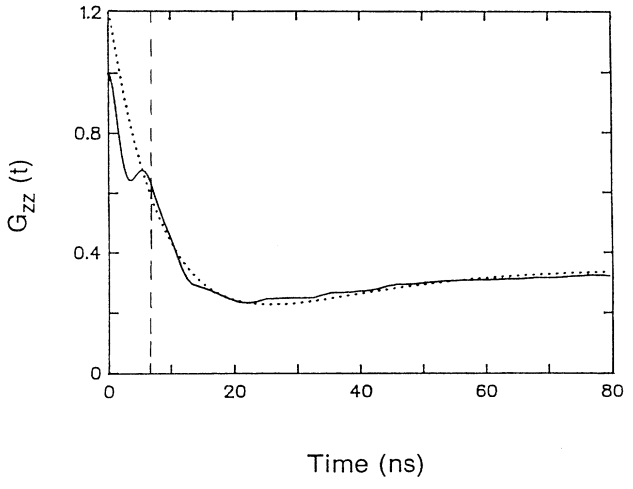

FIG. 7. Monte Carlo static ZF muon spin (polarization) relaxation function generated by the random dipole field distribution at the octahedral interstitial in fcc $Cu_{0.95}Mn_{0.05}$ (solid line), and the least-squares fit of the Lorentzian Kubo-Toyabe relaxation function to the Monte Carlo for times greater than 7 ns (dotted line), as discussed in the text.

lost by use of the continuum approximation can extend beyond the effects of the nearest-neighbor (NN) distance between magnetic moments in solids to nontrivial effects in the next-nearest-neighbor (NNN) distance relative to the first. The two-site alloy effect seems unlikely to be unique to the pure dipolar interaction, because it is the longest-range magnetic interaction, and thus makes a minimum distinction between different distances. Shorter-range interactions will make greater distinction between NN and NNN shell, so the effect may then be enhanced, but the extreme short-range limit is a NN-only interaction, for which the NNN ions, and all further away, are ignored, so the two-site effect must disappear in this limit. The particular example alloy used here may nearly maximize the possible effect for long-range interactions, however, because of the imposed restriction to only one operating interaction and the high crystallographic symmetry. Simultaneous action of two different interactions that both create effective local magnetic fields, or the existence of crystallographically distinct muon sites in the material, are both likely to reduce the effect by filling in the gap between the high- and low-field peaks of the probability distribution. Reduction of the crystallographic symmetry of the muon site should probably be assessed on a case by case basis. The indicative parameter should be a ratio of NNN distance to NN distance, which should be large to generate a large two-site effect, but in some cases the operative NN shell may involve some range of radius from the muon site.

In terms of generating relaxation functions, it would be most convenient if the Monte Carlo field-magnitude distributions could be fit with sums of Maxwellian and magnitude Lorentzians, for then the corresponding static relaxation functions would be known analytically, and the effects of fluctuations could be considered analytically, much of the time. The Maxwellian does fit the Monte Carlo distributions moderately well for concentrations from $x=1.0$ (see top frame of Fig. 2) down to the point where the low-field shoulder begins to be seen, so in that concentration range, $G_{zz}(t)$ should be close to the Gaussian Kubo-Toyabe. In the two-site range, the high-field part always has non-Maxwellian shape, and evolves as concentration decreases toward the single-classical-dipole limit discussed above. The static relaxation function for that limit has been shown by Monte Carlo[18] to execute beating oscillations within a relaxing "envelope" around the $t\rightarrow\infty$ limit value $\frac{1}{3}$. Meanwhile, the low-field part of the magnitude distribution, when it initially emerges near $x=0.3$, is well fit by a Maxwellian, and then an x decreases, seems to evolve in the direction of a more magnitude-Lorentzian shape.

To model line shapes that seem to be between Gaussian and Lorentzian, and quantify relative positions in that range, the Pearson type-VII function is often used.[27] For vector-magnitude probability distributions between Maxwellian and magnitude Lorentzian in shape, a corresponding "magnitude-Pearson" function would be

$$P^{P}(|\mathbf{H}|)=\frac{4\Gamma(b)}{\sqrt{\pi}\Gamma(b-\frac{3}{2})W}\left[\frac{|\mathbf{H}|^2}{W^2}\right]\frac{1}{(1+|\mathbf{H}|^2/W^2)^b}\ , \qquad b\geq 2 \quad (15)$$

where the $b=2$ limit is clearly magnitude Lorentzian, and the $b\rightarrow\infty$ limit is in fact Maxwellian. W here is $\sqrt{b-1}H^*$. Note that $P^P(|\mathbf{H}|)$ is a phenomenological form with no known physical justification. The moments $\langle|\mathbf{H}|^n\rangle$ of this distribution are finite for n less than b, but diverge for $n\geq b$. This functional form fits the low-field distributions well for concentrations down to at least $x=0.15$, with b decreasing from a very large value at $x=0.3$ (i.e., indistinguishable from Gaussian) to $b=9.7$ at $x=0.15$. At $x=0.1$ ($b=7.5$), the fit is only fair, and at $x=0.05$ the fit [shown in Fig. 4(a) for b near 3.5] is poor, so the magnitude-Pearson form fails to reproduce the shape as concentration goes to zero. Meanwhile, the fit value of H^* is also a decreasing function of x. The practical utility of fitting a phenomenological form is greatest if the corresponding static relaxation function is known analytically (not so, here), but no other function was found to fit the low-field-magnitude distribution over its entire concentration range as well as the magnitude Pearson does.

Another way the magnetic alloy situation might be analyzed, motivated by the separation of the effect of the NN shell seen by Monte Carlo, is by studying the effect of fixed-radius shells separately, not just the first (NN), but also second (NNN), third, fourth, etc. out to some radius large enough to apply a continuum approximation beyond that.[18] This possibility has not been investigated in detail.

A real conducting material with such concentrated magnetic moments as modeled here is unlikely to have them both static (on the tens of μ time scale sampled by μSR) and without at the very least short-range order. It may be possible to construct such a system using *nuclear* moments, and then actually observe the relaxation functions of Fig. 3. Somewhat similar ZF μSR has in fact been observed in Y_9Co_7,[28] a material of bizarre crystal structure[29] and poorly understood weak magnetism coexistent with superconductivity at low temperature.[30,31] In that material, the observed variation in the relative intensity of the two signals as a function of temperature is difficult to reconcile with the model of this paper.

V. CONCLUSIONS

Monte Carlo simulation has shown that in polycrystalline alloys involving randomly substituted magnetic ions at concentrations below about 0.3, but not yet in the dilute limit, the field-magnitude probability distribution at a crystallographically unique interstitial (positive muon) site in the magnetically completely disordered state has the form of a two-site distribution. Those sites which have at least one magnetic NN ion generate a high-field peak in the distribution, while those with a completely nonmagnetic NN ion shell generate a distinct low-field peak. Paramagnetic fluctuations of ionic moments would be seen by muons in the two sites as fluctuations *within* the site-separated distributions shown in the site-separated distributions shown in Figs. 2 and 4. For each particular material, the size of the two-site effect is likely to depend on the crystallographic uniqueness of the muon site, the detailed structure of the NN and NNN

ion shells around it, and on the dominance of a single magnetic interaction between muon and ions, which must have range extending at least into the NNN shell. How the finite concentration distributions evolve, as concentration decreases, toward anything like the Lorentzian normally used in the extreme dilute limit, is unclear, partly because the limit distribution, subject to finite ion moments and nonzero minimum separation, is itself not fully understood.

ACKNOWLEDGMENTS

Helpful suggestions were made at various stages of this project by E. J. Ansaldo, J. H. Brewer, M. Celio, S. A. Dodds, and T. M. Riseman. The work was partially supported by the Natural Sciences and Engineering Research Council of Canada, the National Research Council of Canada (via its support of TRIUMF), and Atomic Energy of Canada, Ltd.

[1]For a review, see C. Y. Huang, J. Magn. Magn. Mater. **51**, 1 (1985).
[2]For a review, see J. A. Mydosh, Hyperfine Interact. **31**, 347 (1986).
[3]Y. J. Uemura, T. Yamazaki, R. S. Hayano, R. Nakai, and C. Y. Huang, Phys. Rev. Lett. **45**, 583 (1980).
[4]Y. J. Uemura, D. R. Harshman, M. Senba, E. J. Ansaldo, and A. P. Murani, Phys. Rev. B **30**, 1066 (1984).
[5]Y. J. Uemura, T. Yamazaki, D. R. Harshman, M. Senba, and E. J. Ansaldo, Phys. Rev. B **31**, 546 (1985).
[6]D. E. MacLaughlin, L. C. Gupta, D. W. Cooke, R. H. Heffner, M. Leon, and M. Schillaci, Phys. Rev. Lett. **51**, 927 (1983).
[7]For a review, see J. K. Furdyna and N. Samarth, J. Appl. Phys. **61**, 3526 (1987).
[8]A. Golnick, E. Albert, M. Hanna, E. Westhauser, A. Weidinger, and E. Recknagel, Hyperfine Interact. **31**, 375 (1986).
[9]E. J. Ansaldo, D. R. Noakes, R. Keitel, S. R. Kreitzman, J. H. Brewer, and J. K. Furdyna, Phys. Lett. A **120**, 483 (1987).
[10]E. J. Ansaldo, D. R. Noakes, J. H. Brewer, S. R. Kreitzman, and J. K. Furdyna, Phys. Rev. B **38**, 1183 (1988).
[11]J. Chappert, in *Muons and Pions in Materials Research,* edited by J. Chappert and R. I. Grynszpan (North-Holland, Amsterdam, 1984), pp. 35-62.
[12]L. R. Walker and R. E. Walstedt, Phys. Rev. B **22**, 3816 (1980).
[13]R. Kubo and T. Toyabe, in *Magnetic Resonance and Relaxation,* edited by R. Blinc (North-Holland, Amsterdam, 1967), pp. 810-823.
[14]R. Kubo, Hyperfine Interact. **8**, 731 (1981).
[15]D. R. Noakes, Hyperfine Interact. **31**, 47 (1986).
[16]E. Holschuh and P. F. Meier, Phys. Rev. B **29**, 1129 (1984).
[17]M. Celio, Phys. Rev. Lett. **56**, 2720 (1986).
[18]J. H. Brewer (private communication).
[19]R. E. Walstedt and L. R. Walker, Phys. Rev. B **9**, 4857 (1974).
[20]Y. J.. Uemura and T. Yamazaki, Physica B **109-110**, 1915 (1982).
[21]R. S. Hayano, Y. J. Uemura, J. Imazato, N. Nishida, T. Yamazaki, and R. Kubo, Phys. Rev. B **20**, 850 (1979).
[22]R. Kadono, J. Imazato, K. Nishiyama, K. Nagamine, T. Yamazaki, D. Richter, and J. M. Welter, Phys. Lett. **107A**, 279 (1985).
[23]J. H. Brewer, S. R. Kreitzman, D. R. Noakes, E. J. Ansaldo, D. R. Harshman, and R. Keitel, Phys. Rev. B **33**, 7813 (1986).
[24]J. H. Brewer, D. R. Harshman, R. Keitel, S. R. Kreitzman, G. M. Luke, D. R. Noakes, and R. E. Turner, Hyperfine Interact. **32**, 677 (1986).
[25]M. Gulacsi and Z. Gulacsi, Phys. Rev. B **33**, 3483 (1986).
[26]D. R. Noakes, E. J. Ansaldo, J. H. Brewer, D. R. Harshman, C. Y. Huang, M. S. Torikachvili, S. E. Lambert, and M. B. Maple, J. Appl. Phys. **57**, 3197 (1985).
[27]M. M. Hall, V. G. Veeraraghavan, H. Rubin, and P. G. Winchell, J. Appl. Cryst. **10**, 66 (1977).
[28]E. J. Ansaldo, D. R. Noakes, J. H. Brewer, R. Keitel, D. R. Harshman, M. Senba, C. Y. Huang, and B. V. B. Sarkissian, Solid State Commun. **55**, 193 (1985).
[29]K. Yvon, H. F. Braun, and E. Gratz, J. Phys. F **13**, L131 (1983).
[30]B. V.B. Sarkissian, J. Appl. Phys. **53**, 8070 (1982).
[31]B. V. B. Sarkissian, in *Superconductivity in d- and f-band Metals,* edited by W. Buchel and M. Weber (KFZ, Karlsruhe, 1982), p. 311.